Université de Mons
Faculté Polytechnique – Service de Mécanique Rationnelle, Dynamique et Vibrations
31, Bld Dolez - B-7000 MONS (Belgique)
065/37 42 15 – georges.kouroussis@umons.ac.be

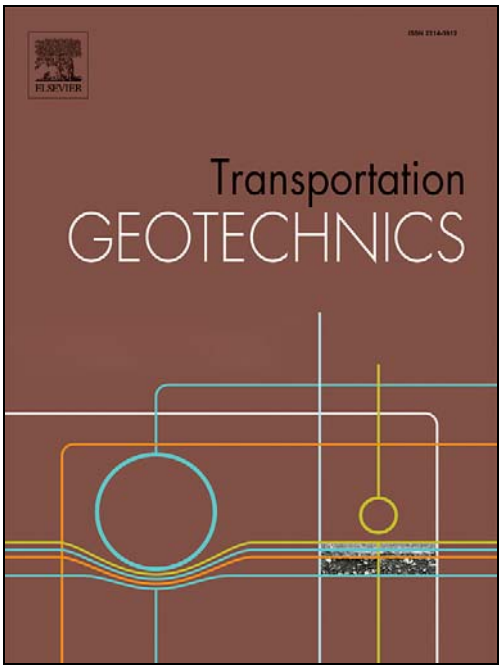

S. Qu, J. Yang, S. Zhu, W. Zhai, G. Kouroussis, Q. Zhang, A hybrid methodology for predicting train-induced vibration on sensitive equipment in far-field buildings, *Transportation Geotechnics*, 31, 100682, 2021.

Transportation Geotechnics 31 (2021) 100682

Contents lists available at ScienceDirect

Transportation Geotechnics

journal homepage: www.elsevier.com/locate/trgeo

A hybrid methodology for predicting train-induced vibration on sensitive equipment in far-field buildings

Shuai Qu [a], Jianjin Yang [a], Shengyang Zhu [a,*], Wanming Zhai [a], Georges Kouroussis [b]

[a] Train and Track Research Institute, State Key Laboratory of Traction Power, Southwest Jiaotong University, Chengdu, China
[b] Department of Theoretical Mechanics, Dynamics and Vibrations, University of Mons, Mons, Belgium

ARTICLE INFO

Keywords:
Environmental impact assessment
Train-induced vibrations
Vehicle-track coupled dynamics
2.5D FEM
Green's function

ABSTRACT

The prediction of train-induced vibration on far-field buildings is a challenging issue in the transportation environment communities. In this work, a hybrid prediction method is put forward utilizing the idea of sub-structure analysis, which can high-effectively calculate the train-induced vibration under different operation conditions. Based on vehicle-track coupled dynamics theory, wavenumber finite element theory (2.5D FEM) and Green's function method, this method could comprehensively analyze vibration characteristics of the source, propagation path and sensitive target/vibration receiver by appropriately considering the boundary conditions between each part. The proposed model possesses the advantages of 2.5D FEM in calculation efficiency and could consider the dynamic interaction between vehicle and track system more elaborately. In addition, the vibration response under different operation conditions can be high-efficiently obtained by updating the track supporting forces without repeatedly solving the Green's functions of the system. On this basis, this work predicts the vibration impact of subway train operation on the sensitive equipment in a far-field large-scale building, and uses the generic vibration criteria for sensitive equipment to evaluate the vibration responses. Further, to mitigate the impact of train-induced vibration, floating slab track is adopted to achieve the vibration attenuation in the concerned frequency. Results show that the train-induced vibration on the monolithic bed track exceeds the limit specified in the standard in some frequency bands. The use of floating slab track can effectively reduce the vibration response of the building and ensure the routine use of sensitive equipment.

Introduction

Among all the recent improvements of underground railways in metropolitan cities, ground-borne vibrations caused by underground trains have long held back in the environmental and transportation communities. In some particular cases, tiny vibrations can disturb the routine use of sensitive equipment. Engineering and scientific communities have paid more attention to this phenomenon and developed several research methods to predict vibration problems caused by subway operation [18,21,29]. These methods include empirical prediction and field test methods [13,15–16,24,34,37], analytical or semi-analytic methods [11,20], sophisticated numerical calculation methods (such as periodic structure method [6], finite element-infinite element method [25], 2.5D FEM [2], 2.5D FEM-BEM [19], 2.5D FEM-IEM [10], 2.5D FEM-PML [17], 2.5D FEM-MFS [1]) and intelligent prediction methods based on deep learning theory [5]. They can well analyze the train-induced vibration effects involved in this phenomenon. The development and application of these models help researchers better understand the mechanism and transmission laws of train-induced vibrations. From the engineering perspective, field tests can accurately obtain the vibration response under actual conditions. However, this method is powerless to predict the train-induced vibration for uncompleted subway lines or buildings. Analytical/semi-analytical and intelligent prediction algorithms are often based on many ideal assumptions, which is not easy to deal with complex configurations and changing dynamic characteristics. In this context, numerical calculation methods could be a more effective tool for handling complex dynamic systems.

Given the shortcomings that the two-dimensional plane model cannot simulate the moving load effect, and the three-dimensional space model is too time-consuming, researchers have proposed the wavenumber finite element method (also called 2.5D FEM). This method assumes the material physical properties and geometry size is constant along the direction of the track. The Fourier transform of time and track direction transform the time–space domain problem into the frequency-

* Corresponding author.
E-mail address: syzhu@swjtu.edu.cn (S. Zhu).

https://doi.org/10.1016/j.trgeo.2021.100682
Received 9 July 2021; Received in revised form 23 September 2021; Accepted 25 October 2021
Available online 30 October 2021

wavenumber domain. The method only needs to consider the two-dimensional section perpendicular to the moving load, significantly reducing the calculation cost while ensuring good accuracy. On this basis, Connolly et al. [4] proposed a new hybrid time–frequency domain method to predict the railway vibration caused by structural defects and its propagation in the track, soil and nearby buildings. Kouroussis et al. [12] conducted a numerical-experimental study based on in-situ transfer functions and simulated vehicle-track results to analyze ground vibration induced by local defects. Triepaischajonsak and Thompson [22] combined the wheel-rail interaction model in the time–space domain and the layered ground model in the wavenumber-frequency domain to form a hybrid model to predict the train-induced ground vibration. Zhu et al. [36] proposed an efficient and robust approach for analyzing the random ground vibration caused by subway trains, combined with the 2.5D FEM-PML (perfectly matched layers) and the pseudo-excitation method. The studies mentioned above provide beneficial solutions in high-efficiently predicting train-induced vibration.

In current engineering applications, it is often essential to predict and analyze the train-induced vibration caused by different operation conditions. Traditional environmental vibration prediction methods will consume unaffordable time for "repetitive calculations". In this regard, based on vehicle-track coupled dynamics theory and 2.5D FEM, this paper proposes a hybrid method suitable for predicting the train-induced environmental vibration under different operation conditions. Compared with the existing researches, the model fully considers the "source-propagation path-sensitive object/receiver" dynamic system and improves calculation efficiency under different train operation conditions by updating track supporting forces. Based on a specific engineering project, the proposed prediction method is used to evaluate the vibration impact of a to-be-built subway on sensitive equipment in a to-be-built large-scale hospital in the far field. The generic vibration criteria for sensitive equipment (VC standard) is used to evaluate the usability of the sensitive equipment interfered with by subway trains. Finally, the effect of the steel-spring floating slab track on alleviating the building vibration is investigated.

Prediction method

Based on the concept of substructure analysis, this paper proposes a prediction method that can efficiently calculate the environmental vibration caused by subway trains under different operation conditions, as shown in Fig. 1. This method can analyze train-induced vibration from three aspects: the vibration source, propagation path, and sensitive object/receiver. It can effectively obtain the response of the entire system by appropriately considering the boundary conditions between each part.

In the process of vibration source analysis, a vehicle-track dynamic interaction model is adopted [31]. This model has been fully verified by a large number of practical engineering applications [9,26,27], which can conveniently consider the excitations generated by the wheel-rail geometric irregularities and internal structural dynamic irregularities, and can further effectively handle the train-track nonlinear problems (such as nonlinear wheel-rail contact, nonlinear train suspension components) that are hard to be resolved by frequency-domain methods.

In the vibration propagation path analysis, it is assumed that the subgrade, tunnel, and soil are continuous and uniform along the track. The 2.5D FEM can be used to realize the conversion from the three-dimensional problem to the plane strain problem [19]. Subsequently, the vibration response of the system under unit impulse excitation (also called Green's function) is calculated. Finally, the vibration response can be efficiently obtained by employing Duhamel integral on track supporting forces and Green's functions.

When predicting the vibration of sensitive objects or receivers, an elaborate FE model of the building is established. The soil vibration is applied as an excitation on the building foundation in an inconsistent manner. Finally, vibration responses at the equipment installed

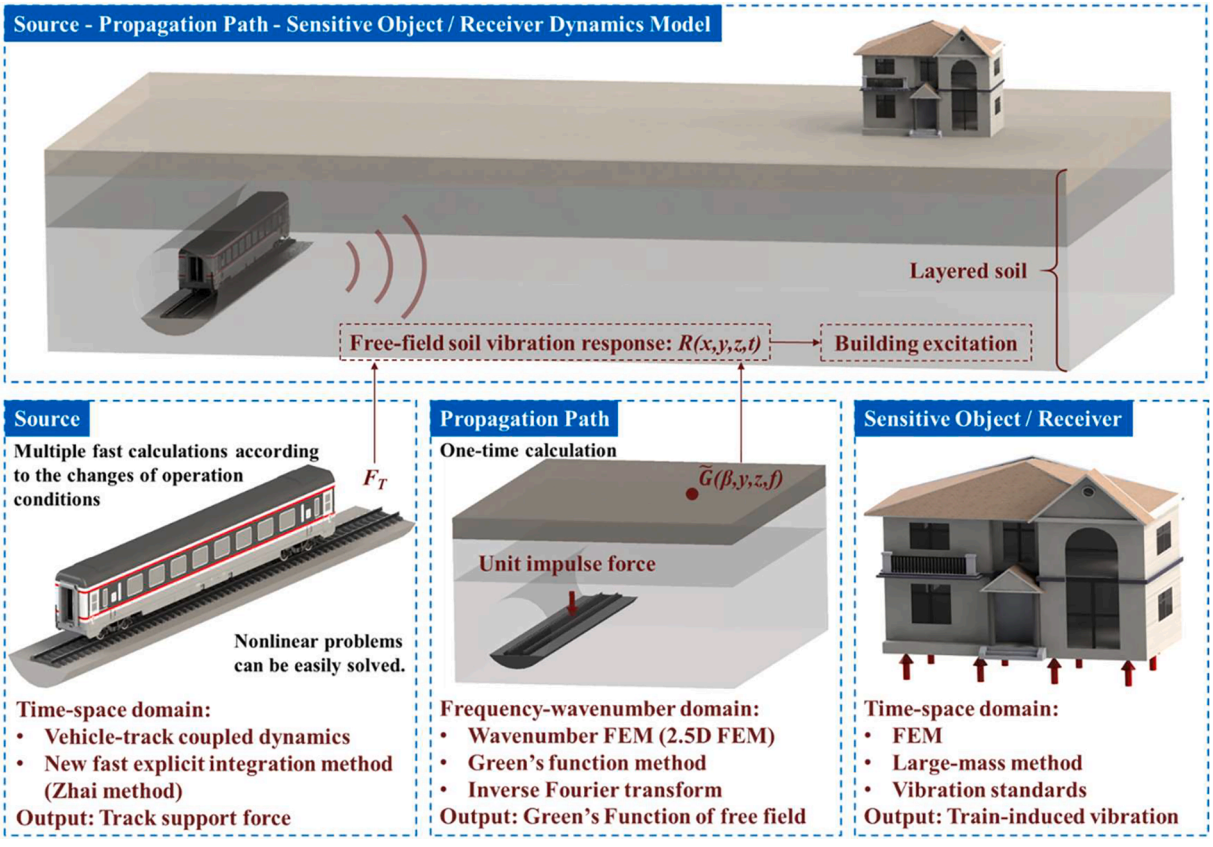

Fig. 1. Schematic diagram of the prediction method.

locations are calculated and compared with the vibration limits to evaluate the environmental vibration impact caused by subway trains.

If the train operating conditions change (such as train formation, running speed, line status, track vibration reduction and isolation measures), it is only needed to update the track supporting forces without repeatedly calculating the Green's functions of the tunnel-soil system to predict the environmental vibration. The calculation for vehicle-track interaction could be very fast by using the explicit fast integration method.

Vehicle-track coupled dynamics model

When a subway train travels along the track, the vibration caused by the vehicle dynamically affects the track structure. Moreover, the vibration of the track structure will cause the change of the wheel-rail contact behaviour, which will lead to the change of vehicle dynamic performance. Therefore, it is necessary to couple vehicles and tracks for the system vibration analysis through the wheel-rail interaction. To effectively simulate the dynamic interaction between vehicles and tracks and evaluate their dynamic performance, a vertical vehicle-track coupled dynamics model is adopted in this work [31,33], as shown in Fig. 2. This model considers the influence of the car body, the front and rear bogies, the wheelsets, and the primary and secondary suspension system, and especially gives full consideration to the dynamic effect between each wheelset and its superimposed impact on the vibration of track components.

The vehicle model is simulated as a multi-rigid-body system, consisting of motor vehicles and trailers. Totally 10 degrees of freedom is considered for each vehicle, including the bounce (Z_c) and pitch (β_c) motions of the car body, the bounce (Z_{t1}, Z_{t2}) and pitch movements (β_{t1}, β_{t2}) of the front and rear frames, and the bounce motion of the four wheelsets (Z_{wi}, $i = 1 \sim 4$), while the dynamic interactions between adjacent car bodies are ignored in this model. Refer to the previous study [14], the motion equations of each vehicle system component can be expressed in the form of a series of second-order differential equations in the time domain.

$$M_V\ddot{Z}_V + C_V\left(\dot{Z}_V\right)\dot{Z}_V + K_V(Z_V)Z_V = F_V\left(Z_V, Z_T, \dot{Z}_V, \dot{Z}_T\right) + F_{EXT} \tag{1}$$

where Z_V and Z_T represent the displacement vectors of the train system and the track system; M_V is the mass of the train system; C_V and K_V are the damping and stiffness matrices of the train system respectively, which are related to the motion status of the vehicle components; F_V is the wheel-rail interaction force, which is related to the displacement and speed of the train and track; F_{EXT} is a load vector composed of additional external forces.

Since train-induced environmental vibration is more concerned with the vibration characteristics of the low-frequency components below 200 Hz, the rail is regarded as a Bernoulli-Euler beam based on elastic point support. The fastener system is simulated as a linear spring-damping element. The rail support points are arranged according to the spacing between actual fasteners, taking into account the vertical freedom degree of the rail. The basement deformation is ignored in the vehicle-track interaction simulation due to its negligible effect. The movement of the rail can be expressed in the form of a fourth-order partial differential equation in the time domain. By introducing the regularised formation of rail motion, and then the fourth-order partial differential equations of the rail can be converted into second-order ordinary differential equations utilizing Ritz's method. Finally, the equations of the track can also be integrated into the standard matrix form like Eq. (1).

$$\boldsymbol{M}_T\ddot{\boldsymbol{Z}}_T + \boldsymbol{C}_T\dot{\boldsymbol{Z}}_T + \boldsymbol{K}_T\boldsymbol{Z}_T = \boldsymbol{F}_T\left(\boldsymbol{Z}_V, \boldsymbol{Z}_T, \dot{\boldsymbol{Z}}_V, \dot{\boldsymbol{Z}}_T\right) \tag{2}$$

where M_T, C_T and K_T are the mass, damping and stiffness matrices of the track system, respectively. F_T is the wheel-rail interaction force. From Eqs. (1) and (2), it can be known that the key point to solving the vehicle-track coupled system lies in the wheel-rail force. The wheel-rail interaction is described in detail in the dynamic wheel-rail coupled model, where the Hertz nonlinear elastic contact theory is employed to determine the wheel-rail contact force.

Vehicle-track coupled dynamics system has several degrees of freedom and strong nonlinearities, such as the wheel-rail nonlinear contact force related to the displacement and velocity of wheel and rail. Therefore, an explicit fast integration method (also known as the Zhai method) is adopted to efficiently solve the numerical integration solution [32]. The integration formula can be written as follows.

$$\begin{cases} Z_{n+1} = Z_n + \dot{Z}_n\Delta t + \left(\frac{1}{2} + \psi\right)\ddot{Z}_n\Delta t^2 - \psi\ddot{Z}_{n-1}\Delta t^2 \\ \dot{Z}_{n+1} = \dot{Z}_n + (1+\varphi)\ddot{Z}_n\Delta t - \varphi\ddot{Z}_{n-1}\Delta t \end{cases} \tag{3}$$

where Z, $\dot{Z}$ and $\ddot{Z}$ represent the displacement, velocity and acceleration, respectively; Δt is the integral time step, and the subscript n means the time at $t = n\Delta t$; φ and ψ are integral control parameters. According to the initial conditions of the system, the dynamic responses of the vehicle and the track system at each moment can be calculated stepwise according to the integral recursive formula.

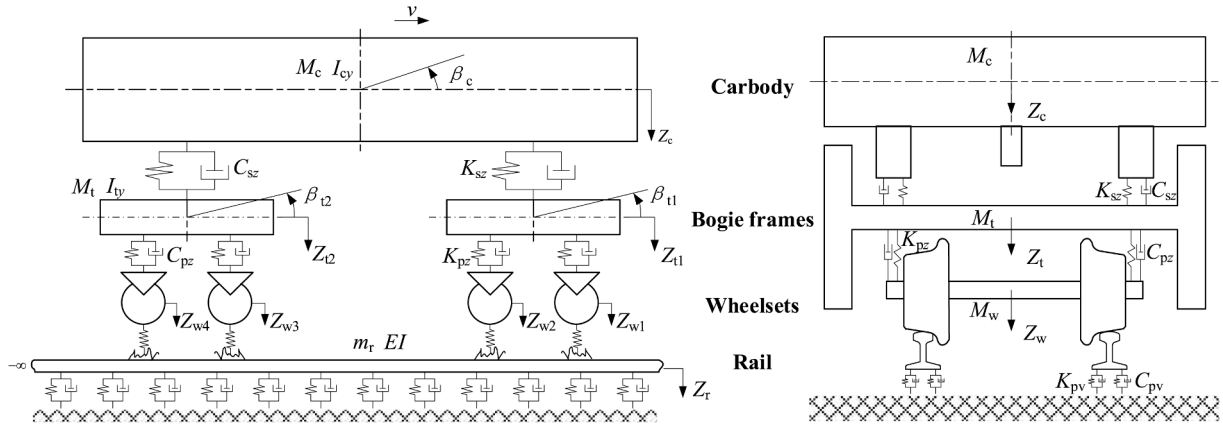

(a) Side view. (b) End view.

Fig. 2. Schematic diagram of vehicle-track coupled dynamics model.

Wavenumber finite element model of tunnel-soil system

The wavenumber finite element method (2.5D FEM) is used to calculate the dynamic interaction between the tunnel and the soil. The three-dimensional dynamic problem is reduced to a two-dimensional plane strain problem through the Fourier transform of the coordinate variables along the track direction. Then the finite elements are discretized and solved in the plane perpendicular to the track. Assuming that the tunnel-soil coupled model is an infinite-length elastic body with unchanged geometry and material properties. All the vibration waves propagating along the track can be discretized into a series of plane waves through FFT, and each plane wave corresponds to a specific wavenumber. Through the inverse FFT of the vibration response under enough wavenumbers, the actual response in the three-dimensional space can be accurately obtained.

The 4-node isoparametric element is adopted to discretize the basement, tunnel and soil perpendicular to the track direction [2]. Each node contains 3 degrees of freedom. The element shape function is expressed as follows:

$$N_i(\eta,\zeta)=\frac{1}{4}(1+\eta\eta_i)(1+\zeta\zeta_i),\qquad (i=1,2,3,4) \tag{4}$$

$$N_i(\eta_i,\zeta_i)=\begin{cases}1 & (i=j)\\ 0 & (i\neq j)\end{cases} \tag{5}$$

where η and ζ are the local coordinates, and η_i and ζ_i are the local coordinates of nodes. Then, the shape function matrix Φ^e of the element can be sorted out.

The relationship between the element displacement deformation u_i, $i=1, 2, 3, 4$, and the element node displacement $\left(u^e_{xj}, u^e_{yj}, u^e_{zj}\right)$, $j=1, 2, 3, 4$ can be expressed as

$$u^e_x=\sum_{j=1}^{4}N_j(\eta,\zeta)u^e_{xj},\qquad u^e_y=\sum_{j=1}^{4}N_j(\eta,\zeta)u^e_{yj},\qquad u^e_z=\sum_{j=1}^{4}N_j(\eta,\zeta)u^e_{zj} \tag{6}$$

For each element, the node displacement vector can be expressed as:

$$\{q^e(x,t)\}=\left(u^e_{x,1},u^e_{y,1},u^e_{z,1},\cdots,u^e_{x,4},u^e_{y,4},u^e_{z,4}\right)^T \tag{7}$$

Then the displacement vector at each point in the element can be expressed as:

$$\{u^e(x,y,z,t)\}=[\Phi^e(x,y,z)]\{q^e(x,t)\} \tag{8}$$

Dividing the cross-sections at x and $x+dx$ into a series of units in the same way, the element A at section x forms the element prism with its corresponding element at section $x+dx$. Substitute the kinetic energy T^e, potential energy U^e and generalized force vector Q^e_j ($j=1, 2, 3, 4$) of the prism element into the Lagrange's equation of the second kind, yielding:

$$\frac{d}{dt}\frac{\partial T^e}{\partial \dot{q}^e_j}+\frac{\partial U^e}{\partial q^e_j}=Q^e_j(1,2,3,4) \tag{9}$$

The differential equation of motion of the element is obtained as [19]:

$$[M^e]\{\ddot{q}^e(x,t)\}+[K^e]_0\{q^e(x,t)\}+[K^e]_1\frac{\partial}{\partial x}\{q^e(x,t)\}-[K^e]_2\frac{\partial^2}{\partial x^2}\{q^e(x,t)\}=\{F^e(x,t)\} \tag{10}$$

Among them, $[M^e]$is the element mass matrix; $[K^e]_0$, $[K^e]_1$, $[K^e]_2$are the element stiffness matrices, and $\{F^e(x,t)\}$ is the element external load matrix. Furthermore, each element matrix can be integrated into the system mass matrix $[\boldsymbol{M}]$, stiffness matrix $[\boldsymbol{K}]_0$, $[\boldsymbol{K}]_1$, $[\boldsymbol{K}]_2$ according to the node position coordinates of the element. Assuming that there are n nodes in the cross-section at the track direction, their displacement and force can be represented by a $3n$ order vector:

$$\{\boldsymbol{q}(\boldsymbol{x},\boldsymbol{t})\}=\left(u_{x,1},u_{y,1},u_{z,1},\cdots,u_{x,n},u_{y,n},u_{z,n}\right)^T \tag{11}$$

$$\{\boldsymbol{F}(\boldsymbol{x},\boldsymbol{t})\}=\left(F^e_{x,1},F^e_{y,1},F^e_{z,1},\cdots,F^e_{x,n},F^e_{y,n},F^e_{z,n}\right)^T \tag{12}$$

Fourier transform can be performed on the system differential equation to obtain the expression in the frequency-wavenumber domain [19]:

$$\left([K]_0+i\beta[K]_1+\beta^2[K]_2-\omega^2[M]\right)\{\widetilde{q}(\beta)\}=[K(\beta)]\{\widetilde{q}(\beta)\}=\left\{\widetilde{F}(\beta)\right\} \tag{13}$$

In the formula, β is the vibration wavenumber (rad/m). Since the dynamic strain of soil caused by subway train operation is generally 10^{-5} m or less, which belongs to the elastic deformation stage. Therefore, it is unnecessary to consider soil nonlinearity in this work, and the soil is regarded as a triaxial homogeneous elastomer. Since the ground is a semi-infinite space in reality, to minimize the influence of boundary reflections caused by the model reduction during the FE modelling process, an artificial viscoelastic boundary needs to be set at the soil boundary. It can be implemented by modifying material properties and constraining the outer nodes of the outermost elements. The material properties of the viscoelastic artificial boundary element are described as those in the reference [28].

Green's function method

Green's function of the system $G(\beta,y,z,f)$ can be obtained when the system is excited by unit impulse excitation, then the result of which in the time–space domain can be obtained by inverse Fourier transform, denoted as $G(x, y, z, t)$. The vibration response $R(x,y,z,t)$ (such as displacement, velocity, acceleration, strain) of each node of the system (x,y,z) can be obtained by the Duhamel integration of the track supporting forces solved in Section 2.1 and the Green's functions obtained in Section 2.2.

$$\begin{aligned}\mathrm{R}(x,y,z,t)&=\sum_{i=-\infty}^{+\infty}\int_0^t G(x,y,z,x_i,y_\mathrm{F},z_\mathrm{F},t-\tau)F_{rsi}(\tau)d\tau\\&=\sum_{i=-\infty}^{+\infty}\int_0^t G_i(x,y,z,t-\tau)F_{rsi}(\tau)d\tau\end{aligned} \tag{14}$$

where $(x_i,y_\mathrm{F},z_\mathrm{F})$ describes the position coordinates of the i th fastener uniformly distributed along the track, $F_{rsi}(t)$ describes the value of the force of the i th fastener at time t; $G(x,y,z,x_i,y_\mathrm{F},z_\mathrm{F},t)$ can also be expressed as $G_i(x,y,z,t)$ to characterize the vibration response of target position (x, y,z) when unit impulse excitation is applied at the i th fastener. Assuming that the tunnel and the soil are uniform in the x direction so that the properties of translation and symmetry can be satisfied:

$$G(x_i+\Delta x,y,z,x_i,y_\mathrm{F},z_\mathrm{F},t)=G\left(x_j+\Delta x,y,z,x_j,y_\mathrm{F},z_\mathrm{F},t\right) \tag{15}$$

$$G(x_i+\Delta x,y,z,x_i,y_\mathrm{F},z_\mathrm{F},t)=G(x_i-\Delta x,y,z,x_i,y_\mathrm{F},z_\mathrm{F},t) \tag{16}$$

Considering that the Green's function will decay with time and distance [3], Eq. (14) can be organized as:

$$\begin{aligned}\boldsymbol{R}(x,y,z,t)&=\sum_{i=-\infty}^{+\infty}\int_0^t G_i(x,y,z,t-\tau)F_{rsi}(\tau)d\tau\\&\approx\sum_{i=-N_\mathrm{F}}^{N_\mathrm{F}}\int_0^{T_c}G_i(x,y,z,t-\tau)F_{rsi}(\tau)d\tau\end{aligned} \tag{17}$$

Where the vibration effects of $2N_F + 1$ fastener forces on the target position are considered in the model, and T_c represents the reduced time.

When the train operation conditions change (vehicle formation, train running speed, line status, train and track vibration reduction and isolation measures, etc.), it is only needed to update the vertical track supporting forces in the first step without solving the tunnel-soil dynamic model repeatedly. And then bring it into Eq. (17) to quickly calculate the vibration response of the system $R'(x,y,z,t)$ under new operating conditions.

Finite element model of building

As shown in Fig. 3, a planned subway line is going to pass near the proposed plot of a hospital that will be equipped with sophisticated equipment for the implementation of proton radiation therapy. This equipment has high requirements for vibration and is likely to be affected by the subway operation. The buried depth of the tunnel is 22.32 m, and the shortest distance between the subway line and the building site is about 123 m. The main building is 88 m long and 54 m wide, divided into above-ground and underground structures. The above-ground structure has ten floors with 46 m high, mainly composed of consulting rooms, wards, offices, and functional rooms; the underground structure has three floors with 17.2 m deep, including equipment installation area, treatment room and office area. This paper focuses on the train-induced vibration impact on the equipment installation location in the building.

The large-scale space between the building and the subway line aggravates the difficulty of solving train-induced dynamic response of the system. The classical theories and methods for solving the environmental vibration caused by subway train operation are no longer applicable. Moreover, similar to the travelling wave effect in seismic vibration, the distances between the subway line and different locations in the building are not the same for large-scale structures in the far field. When a subway train passes, there will be apparent differences in vibration waves transmitted to each location in time and space. To make the numerical simulation as close as possible to the actual force situation, different vibration excitations are applied to the building foundation according to actual distances from the subway line instead of using the same excitation to the entire foundation. The specific process is as follows.

- Firstly, apply full constraints to all nodes in the outermost layer of the building foundation. For the structure calculated in this article, it exists a three-level underground structure, so that in addition to all the nodes on the bottom of the building, it is also necessary to apply excitations to the other four surfaces of the underground foundation. The red arrows show the locations where the excitations should be applied in Fig. 4.
- Secondly, release the degrees of freedom of these nodes in the excitation direction. Define these outermost nodes as structural particles with large mass. (The numerical simulation of the building in this article is achieved in the commercial finite element software ANSYS. We used mass element MASS21 to define the mass of these structural particles.) Generally speaking, the value of mass constant is 10^6 to 10^8 times the overall mass of the finite element model. The purpose of which is to impose inconstant excitations while avoiding excessive structure displacement. In this work, this approach is defined as the "large-mass method".
- Thirdly, the structural excitations ($\boldsymbol{F} = \boldsymbol{M} \cdot \boldsymbol{A}$) obtained by multiplying the mass with the corresponding soil accelerations at these nodes are applied to the building foundation to complete the inconsistent excitation.

It is worth pointing out that the simulation results solved in this manner would be comparatively more conservative from the perspective of engineering practice. And the vibration assessment in this paper is to analyze the train-induced vibration impact on sensitive equipment, so only the critical nodes in the equipment installation area of the building need to be considered.

Evaluation standard

The sensitive equipment is mainly composed of three parts, namely the beam generation system (cyclotron), beam transmission system

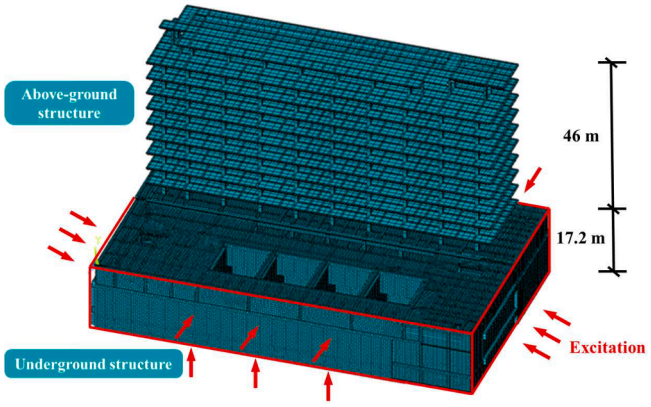

Fig. 4. Finite element model of the building.

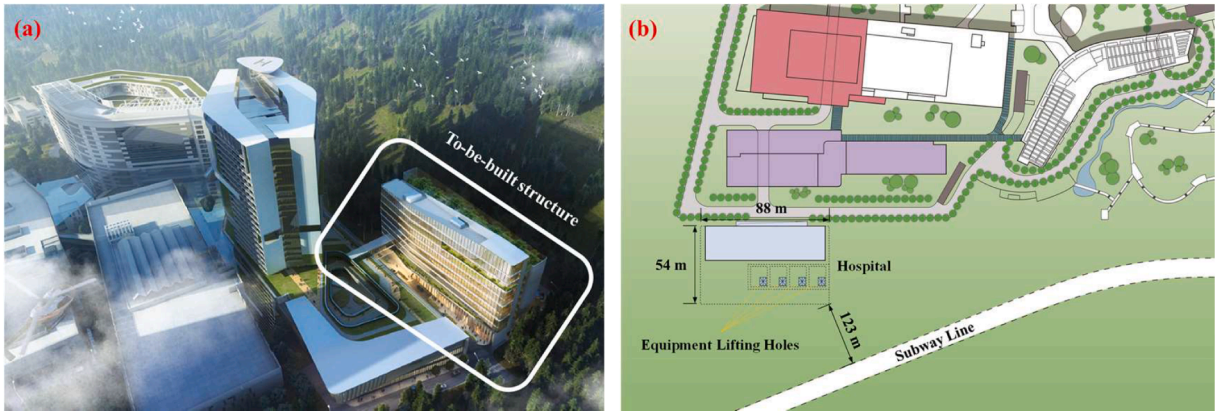

(a) Schematic diagram of to-be-built structure. (b) Location relationship between building and subway.

Fig. 3. Schematic diagrams of the to-be-built project.

(beamline) and beam radiation system (treatment rooms). In the proton therapy system, the protons pass through the cyclotron-energy selector-beam transport line and finally reach the treatment terminal and undergo proton acceleration, injection, energy selection, extraction, and treatment. The schematic layout of the proton therapy system is shown in Fig. 5.

In this project, the train-induced vibration is transmitted to the proton equipment rooms, which may cause the proton equipment to exceed the vibration limit. It not only affects the transportation of the proton current in the beam delivery system but also affects the positioning deviation of the proton beam in the beam radiation system. The generic vibration criteria for sensitive equipment, also known as the VC standard, is used to evaluate whether the routine use of equipment will be affected [7]. The one-third octave standard is theoretically more reasonable, because most environmental vibration signals are random, and the energy average of random signals is more representative than the instantaneous amplitude. The principle can be found in the theory of random processes. At present, the VC standard has become the most widely used international standard for evaluating sensitive equipment and environmental vibration evaluation of laboratory site selection. Table 1 is the general stipulation of the allowable vibration amount of sensitive equipment in VC standard [7]. The calculation process mainly considers the magnitude of the vertical vibration of the equipment installation location under different conditions, and the frequency of primary concern is between 1 and 80 Hz.

Model validation and prediction results

Model validation

In this section, referring to the research on subway environmental vibration in the northern section of Beijing Subway Line 4 [8], the reliability of the model proposed in this work is verified by comparing the calculation results. The center of the subway tunnel is 13.5 m from the ground, and the tunnel lining thickness is 0.3 m. The track is a monolithic bed track, UIC60 rails are supported on the railpads, and the fastener spacing is 0.625 m. The width and height of the concrete track slab are 2.5 m and 0.4 m, respectively. The subway train is composed of six vehicles with a speed of 60 km/h. The American track spectrum (wavelength range 1 ~ 30 m) superimposed with a short-wave irregularity (wavelength range 0.05 ~ 0.99 m) is adopted in the simulation. The vehicle parameters used for the model verification are the same as those in the reference [8]. The soil stratification and related dynamic parameters are described in detail in Fig. 6, where different colors represent different soils. The analysis point locates on the ground at 20 m from the subway line. The comparison of the vertical velocity between the present analysis and the numerical result from Gupta is shown in Fig. 7. It can be obviously found that a good agreement can be identified in terms of the velocity amplitudes, with the maximum value of the former is 1.774×10^{-4} m/s, while the latter is 1.862×10^{-4} m/s, which support the validity of the proposed model in predicting train-induced environmental vibrations. Please note that the only minor difference between the two simulation results is probably attributed to the different prediction models and the possible dynamics parameters such as the loss factor and the track irregularity employed in the calculation.

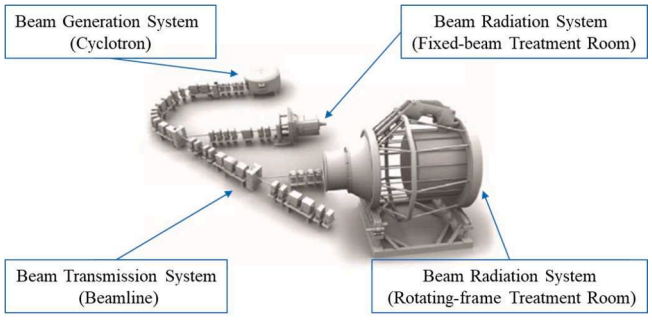

Fig. 5. The schematic layout of the proton therapy system.

Table 1
General regulations for allowable vibration of sensitive equipment.

Vibration Level	Allowable Vibration
VC-A	The acceleration within 4 ~ 8 Hz does not exceed 260 μg. The velocity within 8 ~ 80 Hz does not exceed 50 μm/s.
VC-B	The acceleration within 4 ~ 8 Hz does not exceed 130 μg. The velocity within 8 ~ 80 Hz does not exceed 25 μm/s.
VC-C	The velocity within 1 ~ 80 Hz does not exceed 12.5 μm/s.
VC-D	The velocity within 1 ~ 80 Hz does not exceed 6.25 μm/s.
VC-E	The velocity within 1 ~ 80 Hz does not exceed 3.1 μm/s.
VC-F	The velocity within 1 ~ 80 Hz does not exceed 1.6 μm/s.
VC-G	The velocity within 1 ~ 80 Hz does not exceed 0.78 μm/s.

Dynamic parameters

The train-track interaction is the source of subway system vibration. The weight of the car body is transmitted to wheelsets through bogies, and then to the rail through wheel-rail contact. A typical subway track is the monolithic bed track system (MBT), including rails, sleepers, railpads, fasteners, track beds and foundations. The subway vibration source is closely related to train, track structure, wheel-rail interface irregularities, and running speed. The inertial characteristics, suspension parameters and characteristic length of a subway train are essential for simulating the dynamic response of the system caused by the train operation, as shown in Fig. 8 and Table 2. The subway train comprises six trailers and two motor vehicles located at the front and rear of the train. Axle load is about 17 t when the vehicle is fully loaded.

Because the sleepers and the concrete slab are entirely connected, and there is almost no elasticity between the slab and concrete base, the rail pad provides the main elasticity of the track system. In the simulation, the rail is 60 kg/m, the fastener stiffness is 37 kN/mm, and the sleeper spacing is 0.6 m. The concrete modulus of elasticity of the tunnel and the building is 3.15×10^4N/mm^2. According to the geological survey report, the soil at the site of this project has apparent stratifications. The soil with similar velocities is divided into one layer based on the shear wave speed of each layer. The dynamic characteristics of the in-situ soil layer are shown in Table 3.

In this project, the subway line adjacent to the building is a straight line, and the train is designed to operate at a speed of 120 km/h. The American six-level track spectrum (wavelength 1 ~ 50 m) and short-wave irregularity (wavelength 0.05 ~ 0.99 m) are used to simulate the track geometric irregularity under the subway long-term operation conditions.

Free field vibration caused by train operation

To enable a more comprehensive understanding of the vibration transmission law of this complex system, the vertical ground acceleration and velocity at different distances from the subway are analyzed in the time and frequency domains. The attenuation law of the ground vibration is illustrated in Fig. 9.

The vertical acceleration and velocity peaks can obviously be observed at different ground analysis points when the subway train passes through the building. The influence of each bogie can be identified even at 100 m away from the subway. Table 4 lists the maximum vertical acceleration and velocity of the analysis points at different locations on the ground. It can be found that the amplitude of vibration response decreases with the distance from the subway line. The maximum vertical acceleration of the ground at 20 m from the subway line reaches 6.92×10^{-3} m/s^2. At the subsequent analysis points, the

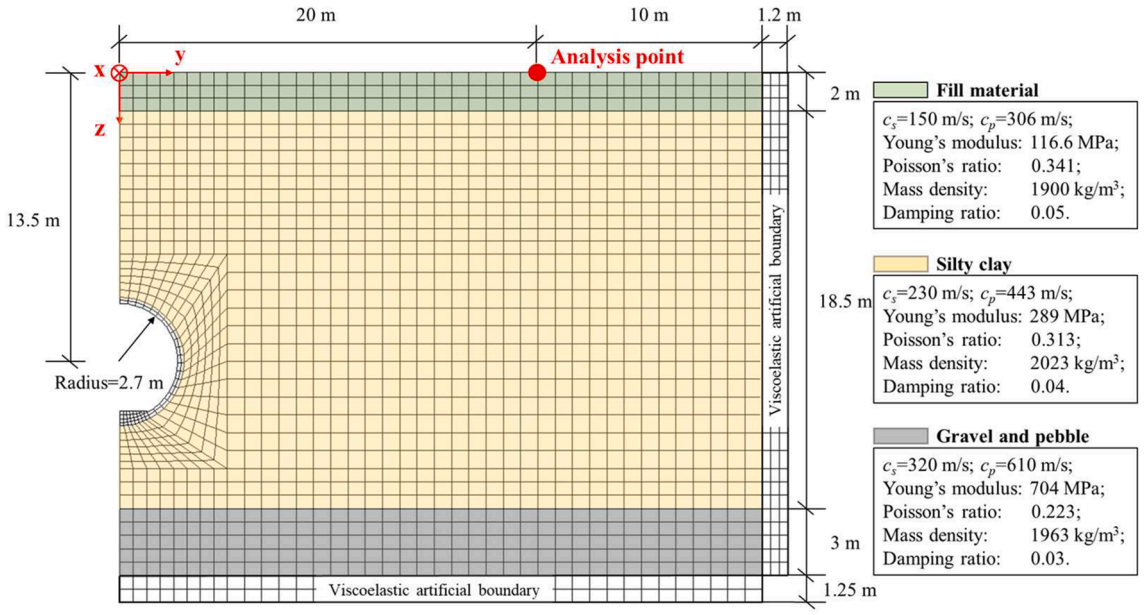

Fig. 6. 2.5D FEM meshes adopted for modelling the tunnel-soil system.

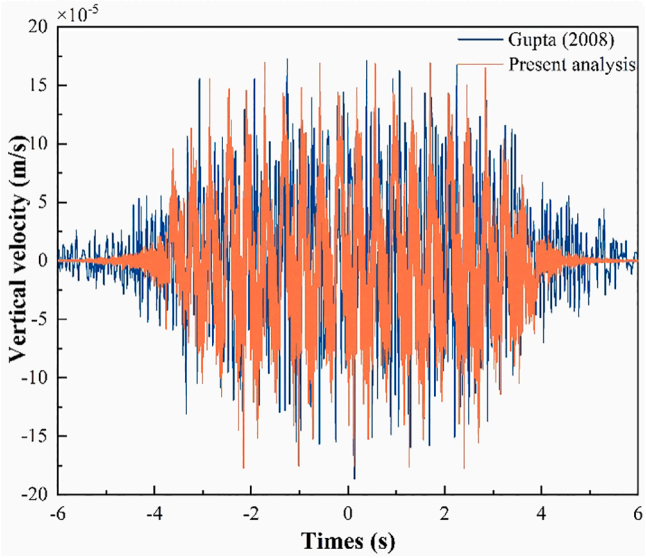

Fig. 7. Comparison of the time history curves of vertical velocity at the analysis point between the analysis by Gupta et al. (2008) and the present analysis.

peaks of vertical vibration acceleration are continuously reduced with an attenuation rate of more than 20%, and the peak of ground vertical acceleration at 100 m attenuates to about 10% of that at 20 m. The variation law of vertical velocity with distance also shows a trend similar to the acceleration. It is worth noting that the vibration response of both vertical acceleration and velocity has a significant attenuation in the range of 20 ~ 40 m and 80 ~ 100 m, with a most reduced rate up to 61.2%. Similar laws have also been mentioned in previous studies [8,16,30,34].

The ground vibration transmission characteristics are further analyzed by converting the ground vibration acceleration and velocity to the frequency domain. It can be found from Fig. 9 that compared to the vertical velocity, the frequency component of the vertical

Table 2
Main parameters of subway vehicles.

Parameters	Motor	Trail	Units
Car body mass (M_c)	49.08	52.22	t
Bogie frame mass (M_t)	4.42	2.39	t
Wheelset mass (M_w)	1.68	1.40	t
Moment of inertia of car body (J_c)	1698.4	1625.4	t•m^2
Moment of inertia of bogie frame (J_t)	4.90	3.45	t•m^2
Primary suspension stiffness (per axle box) (K_p)	1.27	1.27	MN/m
Primary suspension damping (per axle box) (C_p)	26.00	26.00	kNs/m
Secondary suspension stiffness (per bogie) (K_s)	0.27	0.27	MN/m
Secondary suspension damping (per bogie) (C_s)	16.2	16.2	kNs/m

Table 3
Dynamic properties of soil.

Layer	Thickness (m)	Density (t/m^3)	Young's modulus (MPa)	Poisson's ratio	Loss factor
Plain fill	2.0	1.90	117	0.341	0.05
Silty clay	18.0	1.96	289	0.313	0.05
Weathered sandstone	45.4	2.02	704	0.223	0.05

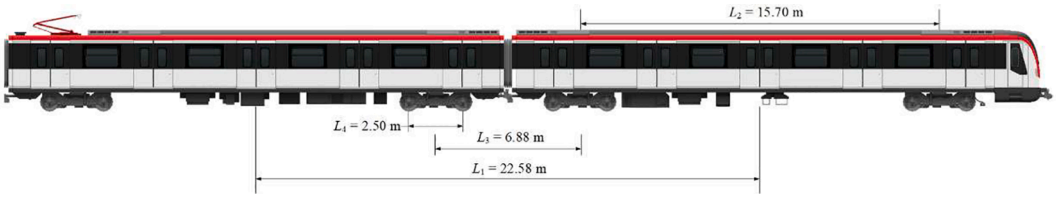

Fig. 8. Characteristic length of the train.

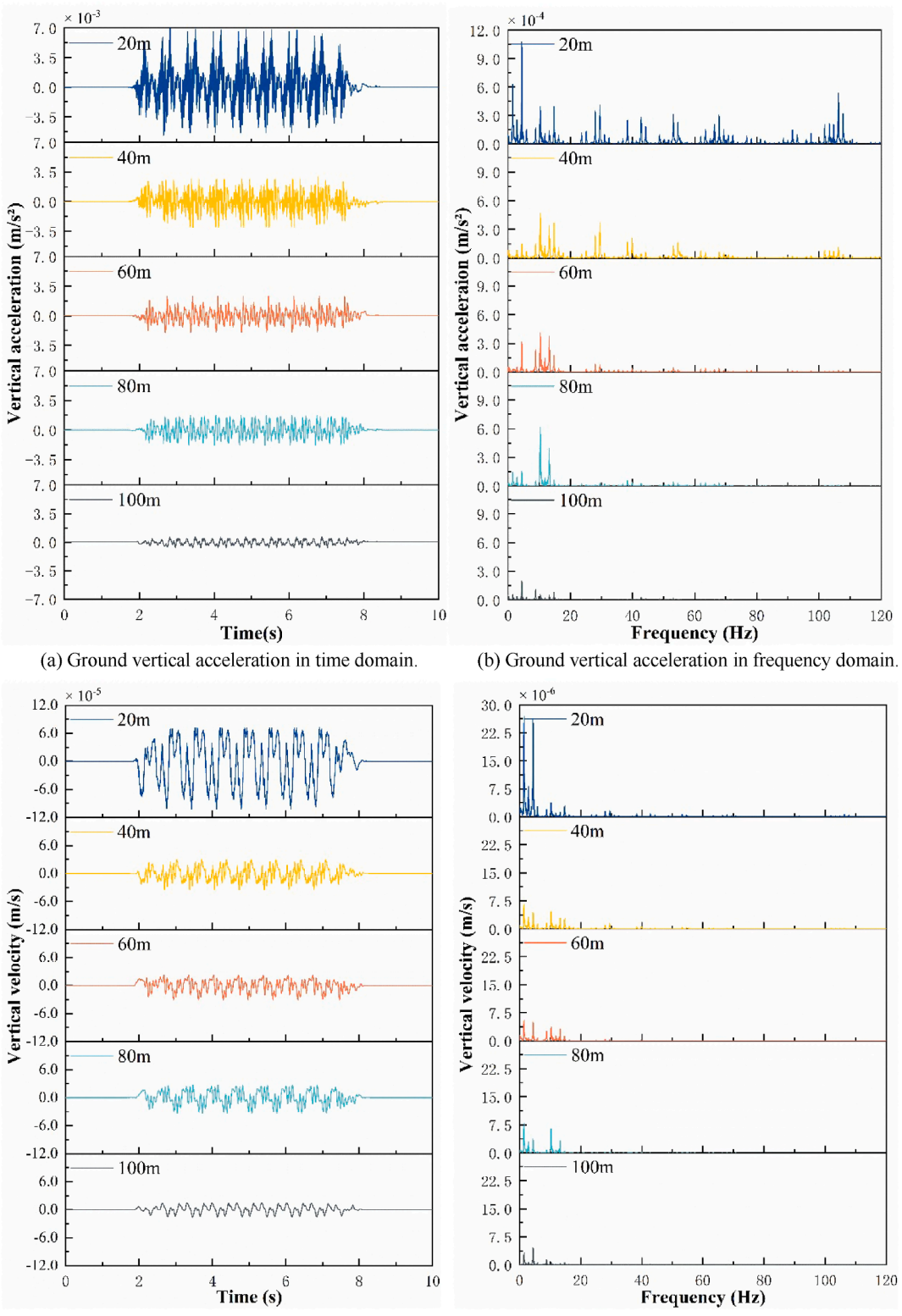

(a) Ground vertical acceleration in time domain.

(b) Ground vertical acceleration in frequency domain.

(c) Ground vertical velocity in time domain.

(d) Ground vertical velocity in frequency domain.

Fig. 9. Ground vibration response at different distances from the centerline of the subway.

acceleration is more abundant, and the frequency components are close to integer multiples of the characteristic frequency of the wheel-rail system, $f_i = v/l_i$, which are mainly caused by the characteristic length of the vehicle, the running speed, the sleeper spacing and the irregular wavelength of the track. The frequency components of the ground vertical velocity are mainly distributed in the range of 0 ~ 20 Hz, and the peaks appear at 1.49 Hz and 4.40 Hz, respectively corresponding to the total length of the vehicle and the distance between adjacent bogies of front and rear vehicles with the subway train running at 120 km/h. At the same time, the frequency components of the ground vertical acceleration and velocity above 20 Hz decay very rapidly as the distance from the centerline increases. The apparent frequency components observed

Table 4
Maximum of train-induced ground vertical vibration.

Maximum value	20 m	40 m	60 m	80 m	100 m
Vertical Acceleration (m/s^2)	6.92×10^{-3}	3.05×10^{-3}	2.32×10^{-3}	1.82×10^{-3}	7.06×10^{-4}
Vertical Velocity (m/s)	7.23×10^{-5}	3.00×10^{-5}	2.32×10^{-5}	2.66×10^{-5}	1.41×10^{-5}

at 100 m from the subway line are mainly distributed within 20 Hz, showing that the low-frequency components play a dominant role in the environmental vibration caused by subway operation in the far field.

Building vibration caused by train operation

According to the hospital architectural drawings and the vibration requirements of the proton equipment, a total of 16 analysis points is selected in the equipment installation area of the third and second underground floors of the building, as shown in Fig. 10. Point 1 is the cyclotron installation node, Points 2 ~ 6 are the critical nodes of the beam transmission system. Points 7 ~ 11 are the foundation installation nodes of the system, Point 12 is the installation node of the fixed-beam treatment room, and Points 13 ~ 16 are the installation nodes of the rotating-frame treatment room. The foundation installation nodes of the system base are directly below the corresponding treatment rooms. The letter "F" is the abbreviation of the foundation, and the letter "TR" stands for the treatment room. In this section, the vibration response of each analysis point in the building is calculated when the subway train passes at a speed of 120 km/h, and no vibration reduction measures are used in this process.

Fig. 11 shows the root mean square (RMS) of the vertical velocity at each analysis point in the one-third octave domain. The figure is marked with grey and black lines for the part that exceeds the VC-F and VC-G vibration limits specified in the VC standard. The vibration response of each analysis point increases first and then decreases as the frequency increases. The vibration peaks are concentrated in the frequency range of 1.6 ~ 2 Hz, 5 ~ 6.3 Hz and 20 ~ 25 Hz, and the corresponding sensitive wavelength range is close to the characteristic length of the vehicle and its integer multiples. Among them, 62.5% of the analysis points in 1.6 ~ 2 Hz exceeds the VC-G vibration limit. All analysis points in the range of 5 ~ 6.3 Hz exceeds the VC-G vibration limit. Moreover, 37.5% of them exceeds the VC-F vibration limit. In the scope of 20 ~ 25 Hz, 37.5% of analysis points exceed the VC-G vibration limit, and one point exceeds the VC-F vibration limit. It can be concluded that the vibration impact of the analysis points caused by the subway train running on the monolithic bed track mainly centralize in the frequency band within 30 Hz. All the analysis points in this frequency band exceed the most stringent VC-G limit in the VC standard, and some analysis points exceed VC-F limit, which may disturb the routine use of proton equipment.

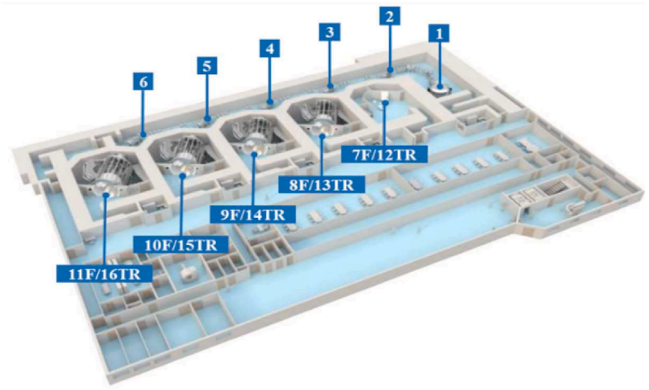

Fig. 10. Selected analysis points in the instrument installation area.

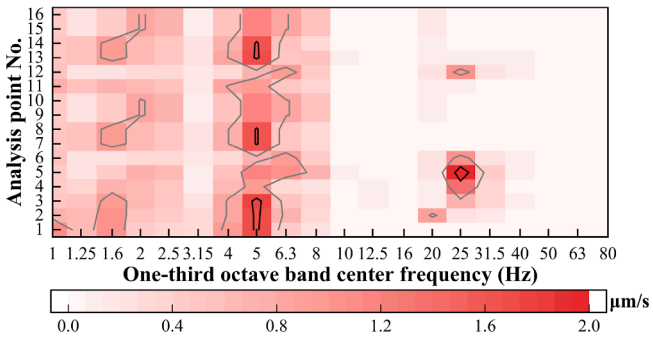

Fig. 11. Vertical velocity levels at analysis points under monolithic bed track.

Vibration reduction analysis

It can be seen from Fig. 11 that referring to the VC standard, the vibration caused by subway train operation exceeds the vibration limit in the standard in the low-frequency range, especially in the 0 ~ 30 Hz frequency range. The RMS of vibration velocity of the proton equipment installation position exceeds the vibration limit of VC-G level, and 43.75% of the analysis points exceed the vibration limit of VC-F level. The proton equipment is an essential means of radiation therapy for cancer patients, the proton flow generation, transmission and radiation in the working process are not allowed to be interfered with by the surrounding vibrations. Although the soil significantly attenuates the vibration induced by train and track interaction during the propagation process, it is found from Fig. 11 that there are still excessive vibrations in some frequency bands. Given that the current calculation only considers the vibration induced by the fully-loaded vehicle without considering the superimposed influence of the planned intercity railways, subway lines and bus lines around the building, it is recommended to adopt steel-spring floating slab tracks (FST) in the subway tunnel to ensure the routine use of the proton equipment.

The FST has been proven to have a good vibration isolation effect in low-frequency ranges and can effectively reduce the vibration transmitted from the track to the tunnel base [23,35]. The floating slab track comprises 60 kg/m rails, fastener systems, floating slabs and steel-spring isolators. The relevant dynamic parameters are given in Table 5. Using the prediction model proposed in this work, the environmental vibration under the new track can be obtained by recalculating the time-history response of the track supporting forces in the train-FST coupled system and perform the Duhamel integration. And there is no need to recalculate the vibration response of the tunnel-soil system, which reflects the high efficiency of this prediction model.

Fig. 12 depicts the results of vertical acceleration at different ground positions in the one-third octave band before and after using the floating slab track. Clearly, when the train runs on the monolithic bed track, the vertical acceleration on the ground shows a gradually decreasing trend with the distance from the subway line. However, slight vibration amplification appears around 2.5 Hz at 60 ~ 80 m from the subway line.

Table 5
Dynamic parameters of steel-spring floating slab track.

Component	Parameters	Values	Units
Slab	Length × width × thickness	24.97 × 4.2 × 0.42	m
	Density	2500	kg/m^3
	Young's modulus	35,000	MPa
	Poisson's ratio	0.25	–
Fasteners Steel	Vertical stiffness	30	MN/m
	Damping ratio	0.2	–
Steel springs	Vertical stiffness	6.6	MN/m
	Damping ratio	0.1	–

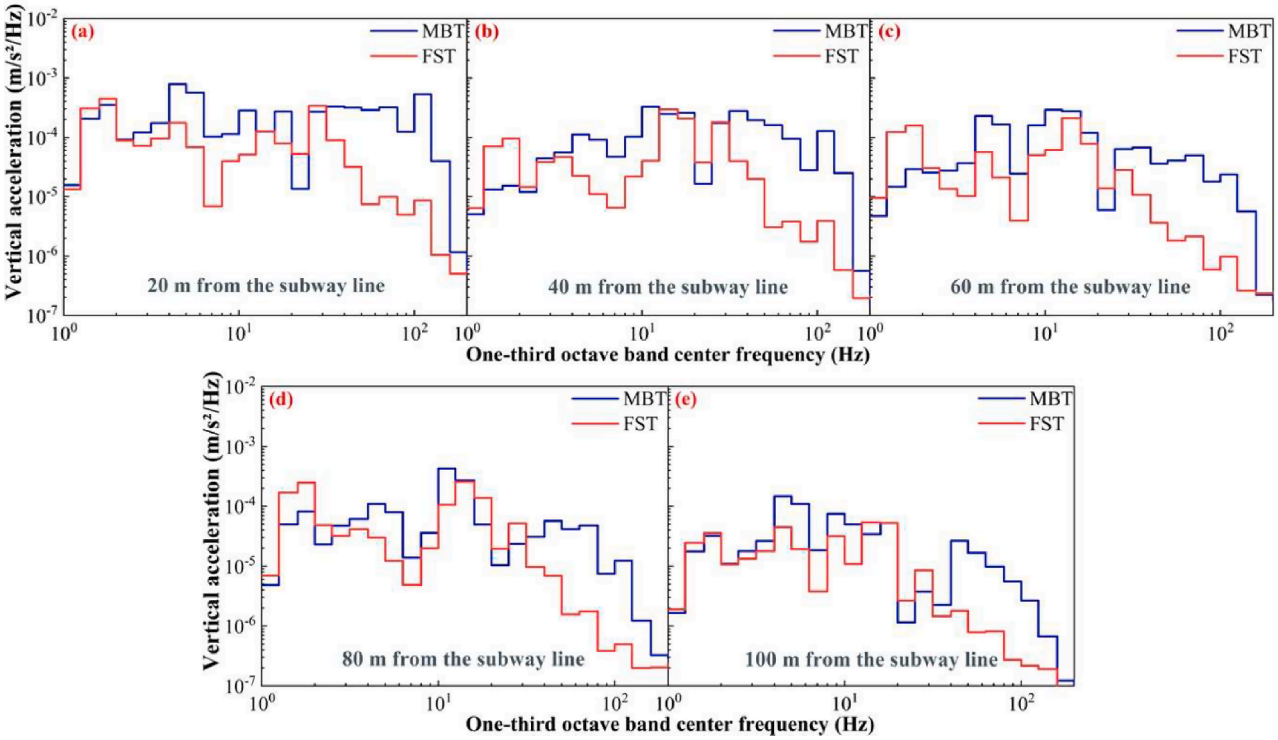

Fig. 12. Vertical accelerations levels at different positions on the ground from the subway line: (a) 20 m, (b) 40 m, (c) 60 m, (d) 80 m, and (e) 100 m.

After adopting the floating slab track, the acceleration variation law at different positions on the ground is the same as using the monolithic bed track. Compared with the monolithic bed track, the vertical acceleration of the ground has a significant vibration reduction effect in the frequency band of 31.5 ~ 200 Hz by adopting the floating slab track. However, there is apparent vibration amplification in the lower frequency band, and the maximum value of some frequency bands even exceeds the vibration response under the monolithic bed track at the same position.

Fig. 13 shows the vibration response of each analysis point in the building in the one-third octave domain after using the steel-spring floating slab track. It can be seen from the figure that after the vibration reduction scheme is adopted, the vibration level of the equipment installation area in the building significantly reduced. The peak value of RMS of the vertical velocity at each analysis point occurs in the range of 20 ~ 40 Hz, which is much lower than the limit value of the generic vibration criteria for sensitive equipment.

In order to illustrate the effect of vibration reduction measures more clearly, Fig. 14 selects representative analysis points (including the beamline installation node, fixed-beam treatment room installation node, rotating-frame treatment room installation node, cyclotron installation node) to make a comparative analysis. Compared with the vibration response under the monolithic bed track, when the subway line is replaced with the steel-spring floating slab tracks, the frequency variation rule of the RMS vibration peak of the vertical velocity does not obviously change while the vibration level is significantly reduced, especially for vibrations within 50 Hz. According to the analysis results in Section 4.3, the vibration response of buildings in the frequency range of 5 ~ 6.3 Hz is the most prominent, and all analysis points exceed the relevant limits of the VC standard. The RMS of vertical velocity is reduced by up to 5 orders of magnitude after using the steel-spring floating slab track. In the other two frequency bands of 1.6 ~ 2 Hz and 20 ~ 25 Hz, the vibration levels are also reduced to 0.01% and 1% of the original vibration level, respectively, which fully ensure that sensitive equipment is not subject to the train-induced vibration.

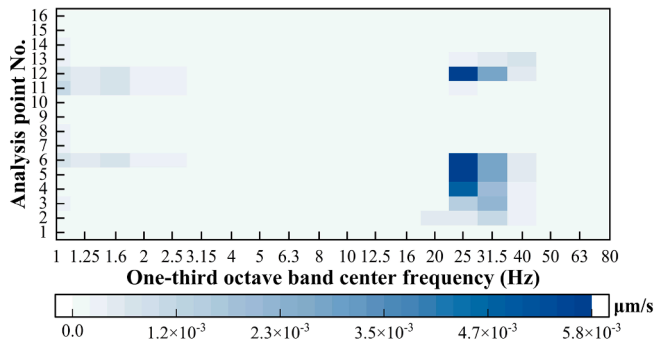

Fig. 13. Vertical velocity levels at analysis points under floating slab track.

Conclusions

This work has proposed a hybrid prediction model for train-induced vibration under different operation conditions. This model possessed the advantages of 2.5D FEM in calculation efficiency and accuracy and could consider more comprehensively the dynamic interaction between vehicle and track, such as the wheel-rail contact nonlinearity and the longitudinal uneven support in track system, which were rather challenging issues for frequency-domain methods. By introducing the Green's function of the system, the vibration response under new operation conditions (changes of the train formation, train running speed, line status, vibration reduction and isolation measures, etc.) could be quickly obtained by updating the track supporting forces without solving the Green's functions repeatedly.

On this basis, this work has evaluated the train-induced vibration impact on the sensitive equipment in a to-be-built hospital in the far field. Further, the effect of floating slab track on controlling the train-induced vibration has been investigated. Main conclusions can be drawn as follows.

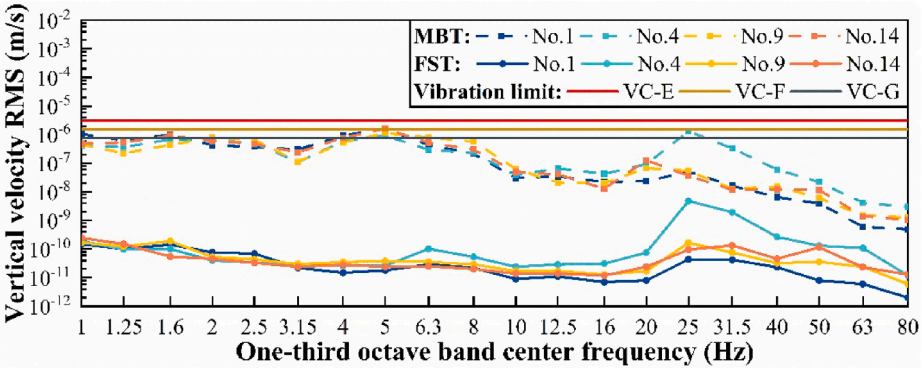

Fig. 14. The RMS of the vertical velocity at some analysis points under MBT and FST. (The dotted line represents the vibration response under MBT, and the solid line represents the vibration response under FST).

(1) The train-induced free-field vibration decreased with the distance from the subway line, while the vibration amplification phenomenon appeared at some position. The vibration attenuation effect in the range of 20 ~ 40 m and 80 ~ 100 m was particularly significant. The ground vibration frequency component at 100 m from the centerline was mainly concentrated within 20 Hz, demonstrating that the low-frequency components are dominant for far-field vibration caused by subway operation.

(2) The vibration of the analysis points in the building caused by the train running on the monolithic bed track exceeded the relevant limits in the generic vibration criteria for sensitive equipment. Especially in the frequency range of 0 ~ 30 Hz, the vibration at the installation position of the equipment was quite severe, indicating that train-induced vibration may affect the routine use of sensitive equipment.

(3) Significant reduction effect of ground vibration can be identified in the frequency band of 31.5 ~ 200 Hz by adopting the floating slab track. However, there was apparent vibration amplification below 10 Hz, and the maximum value of some frequency bands even exceeded the vibration response under the monolithic bed track at the same position.

(4) The steel-spring floating slab track had a significant vibration reduction effect on the building vibrations in the concerned frequency range, which can effectively reduce train-induced vibration on the sensitive equipment in the building.

CRediT authorship contribution statement

Shuai Qu: Conceptualization, Methodology, Software, Validation, Investigation, Data curation, Writing – original draft, Writing – review & editing. **Jianjin Yang:** Conceptualization, Methodology. **Shengyang Zhu:** Funding acquisition, Writing – review & editing, Supervision, Resources, Project administration. **Wanming Zhai:** Funding acquisition, Supervision, Resources, Project administration. **Georges Kouroussis:** Writing – review & editing.

Declaration of Competing Interest

The authors declare that they have no known competing financial interests or personal relationships that could have appeared to influence the work reported in this paper.

Acknowledgements

This work was supported by the National Natural Science Foundation of China (No. 11790283, No. 51978587), the Fund from State Key Laboratory of Traction Power (No. 2019TPL-T16), the China Postdoctoral Science Foundation (No. 2021M692686, No. 2019T120858), and the 111 Project (No. B16041), which is gratefully acknowledged by the authors.

References

[1] Amado-Mendes P, Alves Costa P, Godinho LMC, Lopes P. 2.5D MFS-FEM model for the prediction of vibrations due to underground railway traffic. Eng Struct 2015; 104:141–54. https://doi.org/10.1016/j.engstruct.2015.09.013.

[2] Bian XC, Chen YM, Hu T. Numerical simulation of high-speed train induced ground vibrations using 2.5D finite element approach. Sci. China, Ser. G Physics. Mech. Astron. 2008;51(6):632–50. https://doi.org/10.1007/s11433-008-0060-3.

[3] Chen M, Sun Yu, Zhai W. High efficient dynamic analysis of vehicle–track–subgrade vertical interaction based on Green function method. Veh Syst Dyn 2020;58(7):1076–100. https://doi.org/10.1080/00423114.2019.1607403.

[4] Connolly DP, Galvín P, Olivier B, Romero A, Kouroussis G. A 2.5D time-frequency domain model for railway induced soil-building vibration due to railway defects. Soil Dyn. Earthq. Eng. 2019;120:332–44. https://doi.org/10.1016/j.soildyn.2019.01.030.

[5] Connolly DP, Kouroussis G, Giannopoulos A, Verlinden O, Woodward PK, Forde MC. Assessment of railway vibrations using an efficient scoping model. Soil Dyn. Earthq. Eng. 2014;58:37–47. https://doi.org/10.1016/j.soildyn.2013.12.003.

[6] Degrande G, Clouteau D, Othman R, Arnst M, Chebli H, Klein R, et al. A numerical model for ground-borne vibrations from underground railway traffic based on a periodic finite element-boundary element formulation. J Sound Vib 2006;293(3-5): 645–66. https://doi.org/10.1016/j.jsv.2005.12.023.

[7] Gordon CG. Generic vibration criteria for vibration-sensitive equipment. Optomechanical Engineering and Vibration Control. Int Soc Optics Photonics 1999; 3786:22–33. https://doi.org/10.1117/12.363802.

[8] Gupta S, Liu WF, Degrande G, Lombaert G, Liu WN. Prediction of vibrations induced by underground railway traffic in Beijing. J Sound Vib 2008;310(3): 608–30. https://doi.org/10.1016/j.jsv.2007.07.016.

[9] He Q, Cai C, Zhu S, Wang K, Zhai W. An improved dynamic model of suspended monorail train-bridge system considering a tyre model with patch contact. Mech. Syst. Signal Process. 2020;144:106865. https://doi.org/10.1016/j.ymssp.2020.106865.

[10] Hung HH, Chen GH, Yang YB. Effect of railway roughness on soil vibrations due to moving trains by 2.5D finite/infinite element approach. Eng Struct 2013;57: 254–66. https://doi.org/10.1016/j.engstruct.2013.09.031.

[11] Hussein MFM, Hunt HEM. A numerical model for calculating vibration from a railway tunnel embedded in a full-space. J Sound Vib 2007;305(3):401–31. https://doi.org/10.1016/j.jsv.2007.03.068.

[12] Kouroussis G, Vogiatzis KE, Connolly DP. Assessment of railway ground vibration in urban area using in-situ transfer mobilities and simulated vehicle-track interaction. Int. J. Rail Transp. 2018;6(2):113–30. https://doi.org/10.1080/23248378.2017.1399093.

[13] Lopes P, Ruiz JF, Alves Costa P, Medina Rodríguez L, Cardoso AS. Vibrations inside buildings due to subway railway traffic. Experimental validation of a comprehensive prediction model. Sci Total Environ 2016;568:1333–43. https://doi.org/10.1016/j.scitotenv.2015.11.016.

[14] Luo J, Zhu S, Zhai W. An advanced train-slab track spatially coupled dynamics model: Theoretical methodologies and numerical applications. J Sound Vib 2021; 501:116059. https://doi.org/10.1016/j.jsv.2021.116059.

[15] Mouzakis C, Vogiatzis K, Zafiropoulou V. Assessing subway network ground borne noise and vibration using transfer function from tunnel wall to soil surface measured by muck train operation. Sci Total Environ 2019;650:2888–96. https://doi.org/10.1016/j.scitotenv.2018.10.039.

[16] Qu S, Yang J, Zhu S, Zhai W, Kouroussis G, Zhang Q. Experimental study on ground vibration induced by double-line subway trains and road traffic. Transp Geotech 2021;29:100564. https://doi.org/10.1016/j.trgeo.2021.100564.

[17] Ruiz JF, Soares PJ, Alves Costa P, Connolly DP. The effect of tunnel construction on future underground railway vibrations. Soil Dyn. Earthq. Eng. 2019;125:105756. https://doi.org/10.1016/j.soildyn.2019.105756.
[18] Sheng X. A review on modelling ground vibrations generated by underground trains. Int. J. Rail Transp. 2019;7(4):241–61. https://doi.org/10.1080/23248378.2019.1591312.
[19] Sheng X, Jones CJC, Thompson DJ. Modelling ground vibration from railways using wavenumber finite- and boundary-element methods. Proc. R. Soc. A Math. Phys. Eng. Sci. 2005;461(2059):2043–70. https://doi.org/10.1098/rspa.2005.1450.
[20] Sheng X, Jones CJC, Thompson DJ. A theoretical model for ground vibration from trains generated by vertical track irregularities. J Sound Vib 2004;272(3-5):937–65. https://doi.org/10.1016/S0022-460X(03)00782-X.
[21] Thompson DJ, Kouroussis G, Ntotsios E. Modelling, simulation and evaluation of ground vibration caused by rail vehicles. Veh Syst Dyn 2019;57(7):936–83. https://doi.org/10.1080/00423114.2019.1602274.
[22] Triepaischajonsak N, Thompson DJ. A hybrid modelling approach for predicting ground vibration from trains. J Sound Vib 2015;335:147–73. https://doi.org/10.1016/j.jsv.2014.09.029.
[23] Vogiatzis KE, Kouroussis G. Prediction and efficient control of vibration mitigation using floating slabs: Practical application at Athens metro lines 2 and 3. Int. J. Rail Transp. 2015;3(4):215–32. https://doi.org/10.1080/23248378.2015.1076622.
[24] Xia H, Zhang N, Cao YM. Experimental study of train-induced vibrations of environments and buildings. J Sound Vib 2005;280(3-5):1017–29. https://doi.org/10.1016/j.jsv.2004.01.006.
[25] Xu L, Zhai W. Vehicle–track–tunnel dynamic interaction: a finite/infinite element modelling method. Railw. Eng. Sci. 2021;29(2):109–26. https://doi.org/10.1007/s40534-021-00238-x.
[26] Xu L, Zhai W. Train–track coupled dynamics analysis: system spatial variation on geometry, physics and mechanics. Railw. Eng. Sci. 2020;28(1):36–53. https://doi.org/10.1007/s40534-020-00203-0.
[27] Yang J, Zhu S, Zhai W. A novel dynamics model for railway ballastless track with medium-thick slabs. Appl Math Model 2020;78:907–31. https://doi.org/10.1016/j.apm.2019.09.051.
[28] Yang J, Zhu S, Zhai W, Kouroussis G, Wang Y, Wang K, et al. Prediction and mitigation of train-induced vibrations of large-scale building constructed on subway tunnel. Sci Total Environ 2019;668:485–99. https://doi.org/10.1016/j.scitotenv.2019.02.397.
[29] Yang YB, Hsu LC. A review of researches on ground-borne vibrations due to moving trains via underground tunnels. Adv Struct Eng 2006;9(3):377–92. https://doi.org/10.1260/136943306777641887.
[30] Zhai W, Wei K, Song X, Shao M. Experimental investigation into ground vibrations induced by very high speed trains on a non-ballasted track. Soil Dyn. Earthq. Eng. 2015;72:24–36. https://doi.org/10.1016/j.soildyn.2015.02.002.
[31] Zhai W, Wang K, Cai C. Fundamentals of vehicle–track coupled dynamics. Veh Syst Dyn 2009;47(11):1349–76. https://doi.org/10.1080/00423110802621561.
[32] ZHAI W-M. Two simple fast integration methods for large-scale dynamic problems in engineering. Int J Numer Meth Eng 1996;39(24):4199–214. https://doi.org/10.1002/(SICI)1097-0207(19961230)39:24<4199::AID-NME39>3.0.CO;2-Y.
[33] ZHAI WM, CAI CB, GUO SZ. Coupling model of vertical and lateral vehicle/track interactions. Veh Syst Dyn 1996;26(1):61–79. https://doi.org/10.1080/00423119608969302.
[34] Zhang X, Zhou S, He C, Di H, Si J. Experimental investigation on train-induced vibration of the ground railway embankment and under-crossing subway tunnels. Transp Geotech 2021;26:100422. https://doi.org/10.1016/j.trgeo.2020.100422.
[35] Zhu S, Wang J, Cai C, Wang K, Zhai W, Yang J, et al. Development of a Vibration Attenuation Track at Low Frequencies for Urban Rail Transit. Comput Civ Infrastruct Eng 2017;32(9):713–26. https://doi.org/10.1111/mice:2017.32.issue-910.1111/mice:12285.
[36] Zhu Z, Wang L, Costa PA, Bai Y, Yu Z. An efficient approach for prediction of subway train-induced ground vibrations considering random track unevenness. J Sound Vib 2019;455:359–79. https://doi.org/10.1016/j.jsv.2019.05.031.
[37] Zou C, Wang Y, Moore JA, Sanayei M. Train-induced field vibration measurements of ground and over-track buildings. Sci Total Environ 2017;575:1339–51. https://doi.org/10.1016/j.scitotenv.2016.09.216.